Monthly Notices of the ROYAL ASTRONOMICAL SOCIETY

MNRAS **536,** 266–273 (2025) https://doi.org/10.1093/mnras/stae2522
Advance Access publication 2024 November 8

First on-sky interference fringes at 810 nm with the CHARA array using servo controlled hectometric outdoor fibre links

Julie Magri,[1] Ludovic Grossard,[1]★ François Reynaud,[1] Marc Fabert,[1] Lucien Lehmann,[1] Laurent Delage,[1] Robert Ligon,[2] Norm Vargas,[2] Olli Majoinen,[2] Theo ten Brummelaar,[2] Christopher D. Farrington,[2] Nicholas J. Scott,[2] Narsireddy Anugu,[2] Gail Schaefer,[2] Douglas Gies,[2] Craig Woods,[2] Steve Golden,[2] Victor Castillo,[2] Matt Anderson,[2] Rodolphe Krawczyk[3] and Jean-Michel Le Duigou[4]

[1]*Univ. Limoges, CNRS, XLIM, UMR 7252, F-87000 Limoges, France*
[2]*Georgia State University CHARA Array, Mt. Wilson Observatory, Mt. Wilson, CA 91023, USA*
[3]*Thales Alenia Space, Observation Exploration & Navigation, 5 Allée des Gabians BP 99, F-06156 Cannes La Bocca Cedex, France*
[4]*CNES, Centre Spatial de Toulouse, Service DSO/SI/OP, 18 Avenue Édouard Belin, F-31401 Toulouse Cedex 09, France*

Accepted 2024 November 3. Received 2024 November 3; in original form 2024 April 11

ABSTRACT

In the framework of the ALOHA (Astronomical Light Optical Hybrid Analysis) project, we have implemented a fibre-linked interferometer connecting two telescopes of the CHARA (Center for High Angular Resolution Astronomy) array to the recombination beam facility using servo controlled hectometric outdoor fibres (240 m). During two consecutive nights, on-sky fringes at 810 nm were recorded on the star Vega (mag 0), with servo control of the fibre lengths. The optical path difference was set close to zero using internal fringes found before the on-sky observations. The repeatability of the delay line position offset between internal and on-sky fringes was less than 0.2 mm. The efficiency of the servo control systems has been demonstrated, leading to an enhancement of the signal-to-noise ratio from 68.9 with the servo off to 91.6 with the servo on. This result is a cornerstone for the ALOHA project goal of interferometry at 3.5 µm and a seminal step for the future kilometric infrared fibre-linked interferometer at CHARA.

Key words: instrumentation: high angular resolution – techniques: interferometric.

1 INTRODUCTION

The use of optical fibres for high-resolution imaging in astronomy is a major factor for future very long baseline projects. The original idea was proposed by Connes, Froehly, and Facq (Connes & Reynaud 1988) and mentioned as the solution to the problem of beam diffraction during free propagation between telescopes over hectometre to kilometre distances (Shaklan & Roddier 1987).

Using an outdoor optical fibre link is the only way to envision kilometric baseline telescope arrays for applications in optical astronomy, with angular resolutions in the nanoradian range. For this purpose, we have conducted several studies on the parameters to be controlled when using optical fibres in this coherent context. In 1992, a system of interferometric control of fibre lengths for a coherent telescope array was proposed by Reynaud (Reynaud, Alleman & Connes 1992). A description and laboratory tests of a two-channel prototype for a fibre-linked telescope were reported in 1995 (Alleman, Reynaud & Connes 1995). In 2001, the OHANA (Optical Hawaiian Array for Nanoradian Astronomy) project (Woillez et al. 2001) was proposed at the observatory of Mauna Kea. The goal of the OHANA project was to develop a fibre-linked interferometer in the near infrared using single-mode fibres. In 2005, calibration of silica fibres for the OHANA project was performed with tests on the differential chromatic dispersion evolution as a function of temperature (Vergnole et al. 2005). The OHANA link was successfully used with the two Keck 10 m telescopes without any optical path difference (OPD) stabilization (Perrin et al. 2006). In 2019, stability testing of the optical fibres previously used for the OHANA project was conducted (Lehmann et al. 2019a) at the CHARA (Center for High Angular Resolution Astronomy) array (ten Brummelaar et al. 2005) located at the Mount Wilson Observatory (CA, USA).

Most instruments using optical fibres in the framework of interferometry are in the context of beam combiners, for example MIRC-X (Anugu et al. 2020a), MYSTIC (Setterholm et al. 2023), and SPICA (Mourard et al. 2018) at the CHARA array, or PIONIER (Le Bouquin et al. 2011) and GRAVITY (GRAVITY Collaboration 2017) in the VLTI laboratory.

In this paper, we describe the experimental set-up and the related on-sky results with our 810 nm outdoor hectometric fibre link interferometer implemented at the CHARA array. This study takes advantage of the optical path stabilization reported by Magri et al. (2024). The experimental results presented here are a cornerstone for the future kilometre-sized CHARA Michelson array optical infrared interferometer (Gies et al. 2019; Ligon et al. 2022) and the ALOHA (Astronomical Light Optical Hybrid Analysis) project (Lehmann et al. 2018).

★ E-mail: ludovic.grossard@unilim.fr

2 OVERVIEW OF THE ALOHA PROJECT

The goal of the ALOHA project is to build a mid-infrared (MIR) hectometric fibred, servo controlled, up-conversion interferometer at CHARA. The key stage in this set-up is the up-conversion module that shifts the astronomical light frequency from the MIR to the near infrared (NIR). This takes place at the focus of each telescope and uses a sum-frequency generation (SFG) non-linear process (Boyd 1977). The ALOHA project offers several advantages:

(i) The frequency up-conversion allows us to shift the science signal out of the MIR domain, where the thermal noise makes necessary the use of a cryogenic stage.
(ii) The astronomical light can be transported through optical fibres in the telecommunication spectral window. These precursor tests will also be important for the future expansion of the CHARA Michelson array.

This way, it could be possible to design and implement a kilometric telescope array compatible with the NIR and MIR spectral windows. This ambitious project has been developed step by step during the last two decades. The first in-lab ALOHA proof of concept was demonstrated in 2008 (Brustlein et al. 2008) in the *H* band with a bright artificial source. After in-lab demonstrations in the photon counting regime with a blackbody source (Gomes et al. 2014), the experiment was modified and transported to the CHARA array in 2015. Using the S1 (South 1) and S2 (South 2) telescopes, fringes were obtained on-sky with sources in the *H* band up-converted to visible wavelengths (Darré et al. 2016) with a limiting magnitude $H_{\rm mag} = 3.0$. These successful results in the *H* band convinced us to demonstrate the operation of ALOHA in the *L* band. In this framework, interference fringes were first obtained in the laboratory at 3.39 µm with an attenuated monochromatic coherent laser source (Szemendera et al. 2016). Then, the up-conversion process was validated on one arm of the interferometer during on-sky sensitivity tests in the photon counting regime, reaching a limiting magnitude in the *L* band $L_{\rm mag} = 2.8$ (Lehmann et al. 2019b). These tests were conducted on one of the two telescopes of the C2PU facility (Observatoire de la Côte d'Azur, Calern site, France; https://www.oca.eu/fr/c2pu-accueil). In 2020, an up-conversion interferometer using a blackbody source and a wavefront division in the *L* band at 3.5 µm was demonstrated in the laboratory (Magri et al. 2020). The next step is focused on the implementation and testing of the ALOHA instrument at the CHARA array. This paper presents the experimental interference fringes obtained on-sky at 810 nm using the ALOHA instrument without frequency conversion.

3 FIBRE LINK INTERFEROMETER AT CHARA USING THE ALOHA ARCHITECTURE WITHOUT NON-LINEAR CONVERSION

In order to demonstrate the possibility of using a hectometric outdoor fibre link interferometer at CHARA, the ALOHA set-up was used without non-linear conversion at first. Our instrument installation started in 2019. In March 2022, a mission at the CHARA array focused on the interferometric capabilities of our fibre link, removing the non-linear stage (Fig. 1).

The ALOHA instrument can be divided into two main parts:

(i) The first is a 810 nm astronomical light interferometer.
(ii) The second is a 1064 nm cascade of two metrology systems used to servo control the fibre optical length fluctuations. A Michelson interferometer allows stabilizing the OPD between the two 50 m fibres, used as a reference to feed the two 240 m fibres that propagate the starlight. These two latter fibres then constitute the two arms of a Mach-Zehnder interferometer used to stabilize the OPD.

The overview diagram in Fig. A1 (in the appendix) presents in detail the experimental architecture on the two telescopes. First, the astronomical light is collected by the telescopes S1 and S2. The adaptive optics (AO) systems of each telescope are used to correct the wavefront distortion due to the atmosphere to maximize the flux injection in our set-up (ten Brummelaar et al. 2018; Anugu et al. 2020b). Each light beam is focused by an off-axis parabola and reflected on a tip-tilt mirror before injection into the collecting fibre held by a longitudinal motorized stage. The injection procedure starts with a set of raster scans using the tip-tilt actuator feeding the injection module (which is detailed in Fig. 2). The telescope injection module is longitudinally actuated to place the fibre tip in order to maximize the starlight injection into the 240 m long fibre. The astronomical light coming from the telescopes passes through a dichroic plate, transmitting the signal around 810 nm and reflecting the light at 1064 nm. The astronomical light and the 1064 nm metrology signal are both injected into two 240 m PM fibres going to the recombination laboratory. These fibres are laid outdoors and are protected by insulation foam and PVC pipes.

Fig. A2 (in the appendix) shows the overview diagram of the combining laboratory set-up. The astronomical and metrology lights pass through the collimation module (Fig. 3) placed in the recombination laboratory: the light at the output of the fibre is collimated by an off-axis parabola before passing through a dichroic plate which transmits the 810 nm starlight and reflects the 1064 nm light to be used for metrology purposes. The astronomical light around 810 nm then travels through the free space CHARA delay lines. A moving cart with a cat's eye reflector is positioned on each CHARA delay line to adjust the OPD and compensate for the Earth's rotation. After a round trip in the free space CHARA delay line, the beam is collected by the injection module detailed in Fig. 4 and positioned on the S1 and S2 CHARA beam selection tables. Off-axis parabolas focus the starlight into the two arms of a 810 nm fibre mixing coupler. One arm of the coupler includes a phase modulator, where linear temporal modulation applied by mechanical stretching of the fibre wounded around the piezoelectric ceramic allows displaying the fringes as a function of time. The light is then filtered by a [806–810 nm] bandpass filter in order to increase the coherence length and easily find the fringes. A linear polarization is selected by a polarizer placed before a photon counting detector. An acquisition system is used to record the interferometric signals in the photon counting regime. The fringe pattern is finally Fourier transformed and the power spectral density (PSD) is used to measure the signal-to-noise ratio (SNR) and fringe contrast (Magri et al. 2020).

Simultaneously, a cascade of metrology systems using a very long coherence length laser diode at 1064 nm has been implemented in order to stabilize the OPD between the two 240 m long fibres. This laser is only used for metrology in this configuration without non-linear conversion, but will be used for both metrology and up-conversion when using PPLN crystal conversion stages.

First, the metrology laser beam is shared between S1 and S2 by a 50/50 optical coupler and 50 m optical fibres laid outdoor on the ground and protected by insulating foam and PVC pipes. The 50 m long fibres pass through the telescope cable wrap to reach the optical tables for the AO systems that are mounted on each telescope. This stage needs special attention to limit the variable stress applied to the fibres. In order to manage the optical path fluctuation resulting from the vibrations, mechanical stress and temperature variations, a two-stage actuator, including a fibre

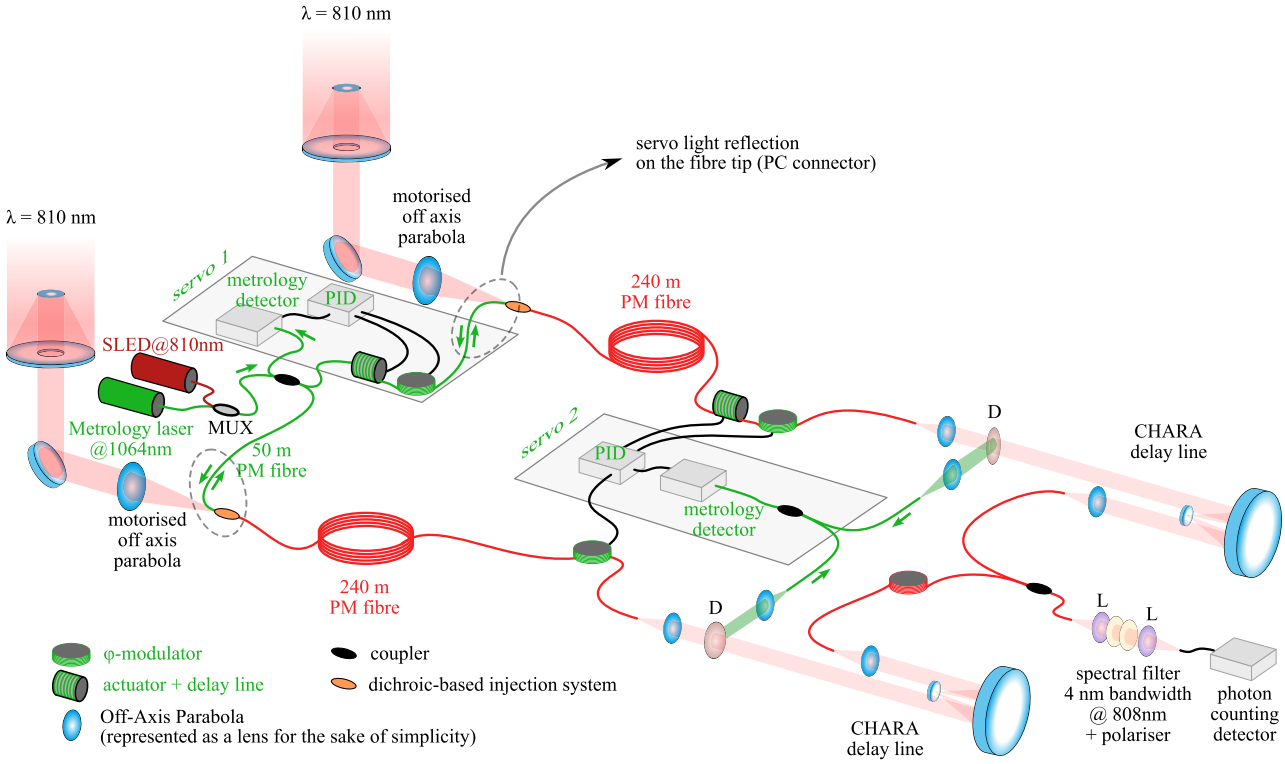

Figure 1. ALOHA at CHARA without the conversion stage: the astronomical light collected at 810 nm and the 1064 nm metrology laser beams are injected into the optical fibres thanks to dichroic plates (not shown here). Off-axis parabolas are represented here as lenses, for simplicity's sake. The metrology light first passes through 50 m long PM fibres. Then the metrology light and the astronomical light propagate in 240 m long PM fibres towards the CHARA free space delay lines. The interferometric mixing is then spectrally filtered by a 4 nm-bandwidth filter in order to increase the coherence length to easily find the fringes. The signal is finally recorded by a photon counting detector. Two cascaded servo control systems (in green in the figure) stabilize the OPD of the pump and astronomical signal fibres. D: dichroic plate to extract the metrology signal, SLED: broad-band superluminescent diode (internal source) used for searching the zero OPD (see Section 4), φ-modulator: fast servo loop phase modulator to servo control the fiber length (in green) or to display the fringe pattern as a function of time (in red), PID: proportional-integral-derivative controller to drive the actuator and φ-modulators, MUX: multiplexer.

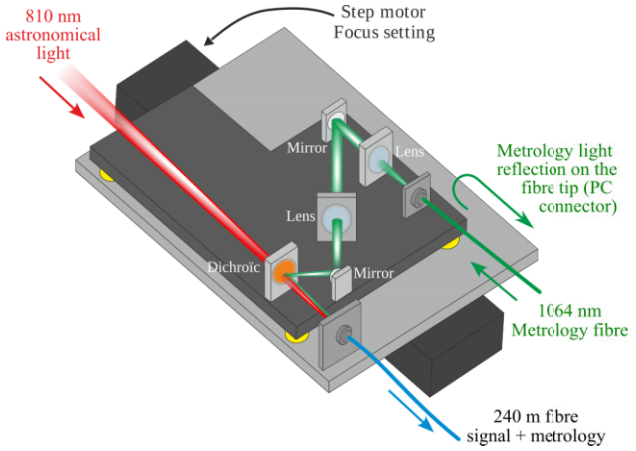

Figure 2. 3D scheme of the injection module in each telescope, without frequency conversion. The astronomical light at 810nm collected by the telescope and the 1064 nm metrology signal are both injected into a 240 m PM fibre going to the recombination laboratory.

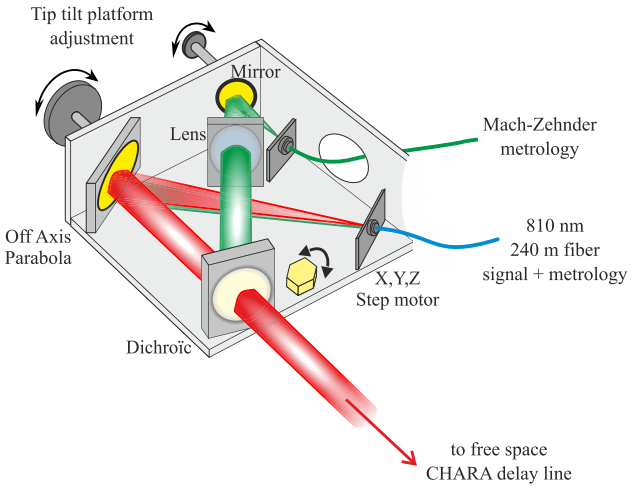

Figure 3. 3D scheme of the collimation module at the entrance of the free space delay line. The astronomical light around 810 nm travels through the free space CHARA delay line whereas the 1064 nm signal is extracted thanks to a dichroic plate for metrology purposes.

delay line and a phase modulator, is implemented on one of the two 50 m long fibres. The servo control for the OPD of the 50 m long fibres has a Michelson interferometer architecture as discussed by Magri et al. (2024). The error signal is provided by the interferometric signal and processed by a proportional-integral-derivative (PID) filter. The resulting correction signal feeds a high voltage amplifier and drives a fibre piezoelectric modulator in a fast servo loop (0.2 ms response time, 3 nm RMS accuracy). In parallel, a fibre delay line driven by a motorized actuator is

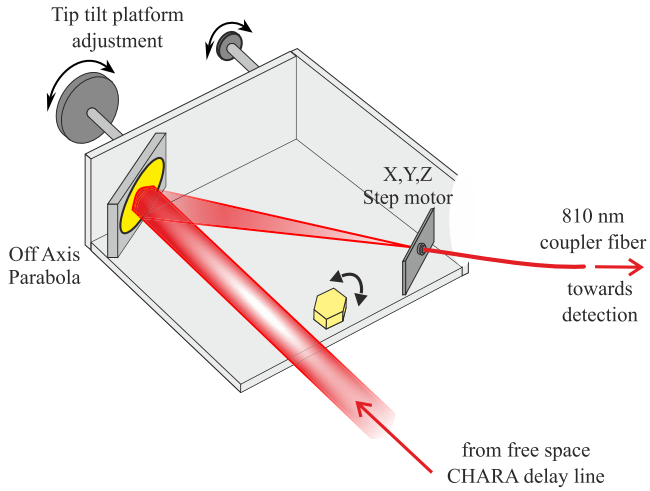

Figure 4. 3D scheme of the injection module at the output of the free space delay line. After a round trip in the free space CHARA delay line, the beam is injected into the recombination coupler.

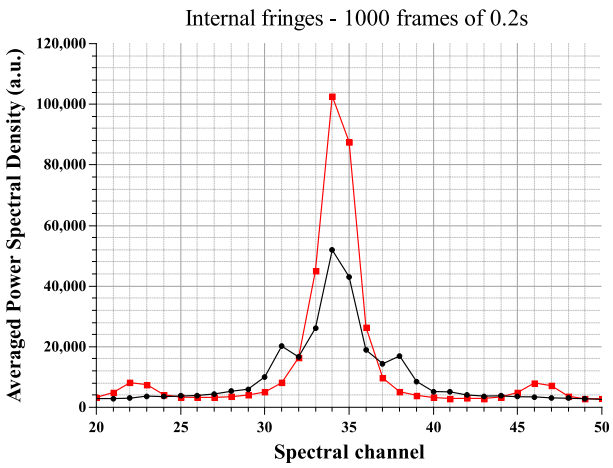

Figure 5. Internal fringe peak, with and without servo control of the length of the optical fibres, during 1000 frames of 0.2 s. The internal source used is a SLED at 810 nm.

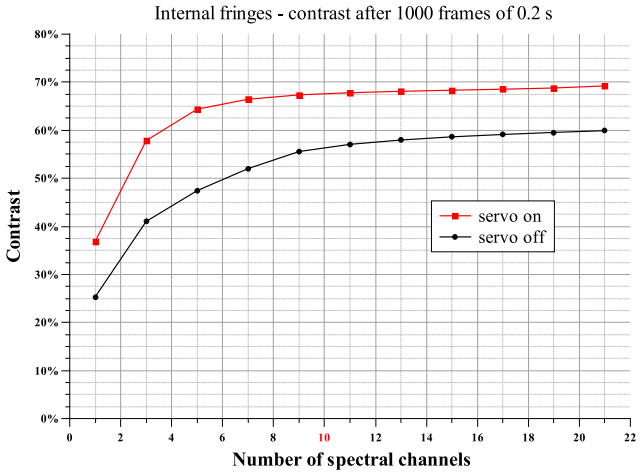

Figure 6. Contrast of the internal fringes with and without servo control as a function of the number of spectral channels used to integrate the fringe peak on either side of the spectral channel 35. The fringe peak was first temporally integrated over 1000 frames of 0.2 s. The internal source used is a SLED at 810 nm. The instrumental contrast is equal to 68 per cent and has been obtained from the internal fringes when the servo control system is on, by integrating the fringe peak over 10 spectral channels. Since the curves were obtained from a single data set, we were not able to derive error bars.

used to desaturate the piezoelectric modulator in a slow servo loop.

A Mach-Zehnder interferometer is used for the metrology stage of the 240 m fibres (Magri et al. 2024). The metrology laser light at 1064 nm is injected into each 240 m long fibre thanks to a set of lenses, mirrors and a dichroic plate placed on the telescope injection module, as shown in Fig. 2. Note that for the future ALOHA project, a PPLN crystal will be placed after the dichroic plate for the frequency up-conversion with the same module footprint on the telescope optical board. After passing through the 240 m long fibre, the metrology light is injected into the collimation stage as detailed in Fig. 3. It is then reflected by a dichroic plate on each arm in the collimation module. The two beams at 1064 nm are mixed by a coupler and the interferometric signal is used as the error signal. After processing by a PID filter and amplification, the correction signal drives a fibre delay line and two phase modulators included on each arm of the interferometer and working in push–pull mode. The two-stage servo control system is operated in the same way as in the Michelson metrology interferometer.

Fig. A3 (in the appendix) shows the set-up installed in the telescope stage at CHARA during the mission in March 2022.

4 INTERNAL FRINGES

In order to find the fringes on-sky, we estimate in a first step the zero group delay position by calibrating the OPD from the telescope foci, passing through the 240 m long fibre sections and the CHARA delay lines, to the interferometric combination. The 50 m long fibres are used to share an internal broad-band source (SLED) around 810 nm between the two telescopes. The high accuracy of the fibre length equalization during the manufacturing process leads to an OPD offset on the order of few mm. The light emitted around 810 nm by the internal source propagates into the two 50 m and 240 m long fibres, passes through the CHARA free space delay lines and reaches the recombination coupler. The fringes are displayed as a function of time using the fibre optical path modulator of the recombining ALOHA set-up. Fringes are processed through a PSD analysis and the fringe peak is centred at 175 Hz. Each 200 ms frame is Fourier transformed and the averaging process is performed on the PSD to fit the on-sky procedure.

The optical servo control system can be either switched on or off in order to demonstrate the fringe contrast improvement due to the optical path stabilization. As the flux emitted by the SLED source is very high, the internal fringes can be found very easily and quickly. The measurement of the internal fringes PSD is shown in Fig. 5. These results highlight the influence of the servo control on the internal fringes (Magri et al. 2024). Phase noise induced by the fibre perturbations is corrected by the metrology servo loop in the internal fringe configuration. It results in a sharper fringe peak and enhanced SNR. The contrast values are obtained from the ratio between the fringe peak integral and the PSD value at the zero frequency (Magri et al. 2020). Fig. 6 plots the evolution of the contrast as a function of the number of spectral channels used to integrate the fringe peak.

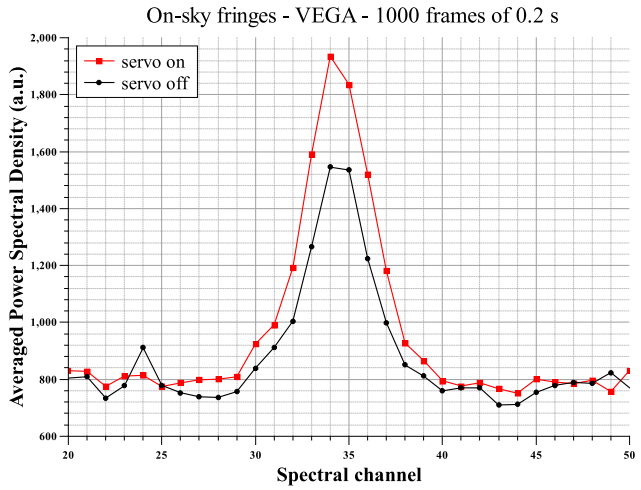

Figure 7. On-sky fringe peak on Vega, with and without servo control of the length of the optical fibres, after integrating over 1000 frames of 0.2 s.

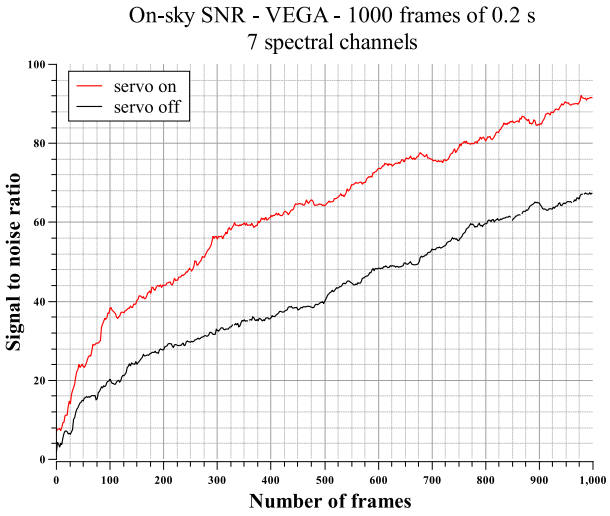

Figure 8. Signal-to-noise ratio of the on-sky fringes on Vega with and without servo control as a function of the number of frames. The fringe peak is integrated over seven spectral channels.

The contrast increases more quickly and reaches a higher value when the servo is on (contrast = 65–70 per cent) in comparison with the servo off configuration (contrast = 55–60 per cent). The instrumental contrast is equal to 68 per cent and has been obtained from the internal fringes when the servo control system is on, by integrating the fringe peak over 10 spectral channels.

5 ON-SKY FRINGES

The measurements presented in this section were obtained during the night of 2022 March 25 to March 26 between 5:40 and 5:46 am (local time) with the star HD172167 (Vega). The atmospheric coherence length r_0 at 550 nm was estimated at 7 cm, corresponding to a moderate seeing of approximately 1.6 arcsec. The photometric levels on the S1 and S2 arms were 2100 and 1100 photons s^{-1}, respectively. The fringe frequency was set to 175 Hz corresponding to a fringe peak centred around channel 35 (i.e. 35 fringes per frame) in the PSD graph. At the observing time, Vega's theoretical contrast at 808 nm (central wavelength of the spectral filter at the end of the instrument chain) for a 34.0 m projected basis is around 57 per cent (calculated using the uniform disc model; Lawson 2000). The position of the internal fringes was first determined before scanning for fringes on Vega. We scanned for fringes with the CHARA delay lines by moving S1 cart with a speed of 70.7 $\mu m\,s^{-1}$ by keeping S2 as reference. Given that we transport light via optical fibres, the CHARA standard baseline OPD solution employed for regular on-sky observations proves ineffective. Instead, we have used the optical fibre transport baseline solution configuration in the Optical Path Length Equalizer server.

The on-sky fringe PSD is plotted in Fig. 7 with servo control on and off. The height of the fringe peak is greater when the servo is on. The influence of the servo control systems is less significant on-sky compared with the internal fringes (Fig. 5) as the phase and intensity noise of the atmospheric turbulence has a large impact at 810 nm and dominates the other sources of noise. As a result, the fringe peak is more spread out and shows a smaller difference in height between the two peaks with and without servo control.

The servo control improves the SNR (Fig. 8) with an SNR equal to 91.6 with the servo on and 68.9 with the servo off after integration during 1000 frames of 0.2 s. The fringe peak is integrated over seven spectral channels.

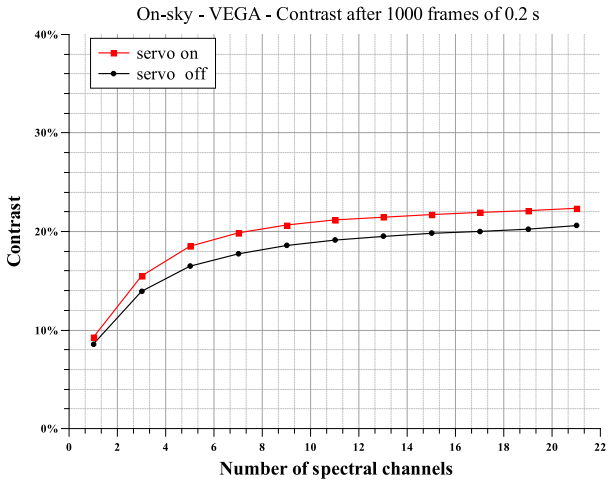

Figure 9. Contrast of the on-sky fringes with and without servo control as a function of the number of spectral channels. Integration time: 200 s. Since the curves were obtained from a single data set, we were not able to derive error bars.

Fig. 9 shows the contrast obtained by integration as a function of the number of spectral channels of the PSD. The fringe contrast obtained on-sky was equal to 22 per cent with the servo control on (taking the photometric imbalance into account). The contrast value corrected from the instrumental contrast reaches 22 per cent ÷ 68 per cent = 32 per cent (measured fringe contrast/instrumental contrast). The ratio between this measurement and the 57 per cent theoretical contrast of Vega is equal to 56 per cent, mainly due to the phase and intensity fluctuations resulting from the atmospheric turbulence.

Using this protocol, we were able to find the fringes on Vega during two consecutive nights. From the first night to the next one, the length difference between the two 240 m long fibres has changed by 2 mm. This shift has been determined and compensated by moving the S1 cat's eye cart in order to retrieve the internal fringes. When we started on-sky measurements, we had to move the S1 cart from the position obtained for the internal fringes by only 0.2 mm to find the on-sky

fringes back. These results are very promising for the future use of fibre links at the CHARA Array and more generally for very long baseline interferometers.

6 CONCLUSION AND PROSPECTS

During our mission in March 2022 at the CHARA array, we were able to find fringes on-sky with our outdoor hectometric fibre link servo controlled interferometer at 810 nm by using the interferometer of the ALOHA project (without the non-linear up-conversion stage).

Our servo control system allows stabilizing the OPD between the 240 m long fibres (with an accuracy of 3 nm) (Magri et al. 2024). The protocol to find fringes on-sky starts by searching for the internal fringes. This way, we were able to find the fringes for the star Vega during two consecutive nights. The 240 m long fibre length difference from one night to the other were less than 2 mm and compensated with the internal fringe procedure. The delay line position repeatability was better than 0.2 mm for the on-sky fringes. We measured an SNR equal to 91.6 with the servo on and 68.9 with the servo off when integrating the fringe peak over seven spectral channels. This result was obtained with only a 200 s integration time. The on-sky contrast value corrected for the instrumental contrast reaches 32 per cent, with the servo control on, taking the photometric imbalance into account. Due to the atmospheric turbulence, the ratio between this measurement and the 57 per cent theoretical contrast of Vega is equal to 56 per cent.

These results are part of the first step for the ALOHA project at 3.5 µm. During a future mission, we plan to test the interferometer with the up-conversion of the mid-infrared light at 3.5 µm. These results are also a first step for the future kilometric infrared fibred interferometer at CHARA. More generally, this experiment paves the way for very long baseline interferometers using fibre optic links.

ACKNOWLEDGEMENTS

This work has been financially supported by the Centre National d'Études Spatiales (CNES), Thales Alenia Space, and the Institut National des Sciences de l'Univers (INSU).

This work is based upon observations obtained with the Georgia State University Center for High Angular Resolution Astronomy Array at Mount Wilson Observatory. The CHARA Array is supported by the National Science Foundation under grants AST-2034336 and AST-2018862. Institutional support has been provided from the GSU College of Arts and Sciences and the GSU Office of the Vice President for Research and Economic Development.

DATA AVAILABILITY

The data underlying this article will be shared on reasonable request to the corresponding author.

REFERENCES

Alleman J. J., Reynaud F., Connes P., 1995, Appl. Opt., 34, 2284
Anugu N. et al., 2020a, AJ, 160, 158
Anugu N. et al., 2020b, in Tuthill P. G., Mérand A., Sallum S., eds, Proc. SPIE Conf. Ser. Vol. 11446, Optical and Infrared Interferometry and Imaging VII. SPIE, Bellingham, p. 1144622
Boyd R. W., 1977, Opt. Eng., 16, 166563
ten Brummelaar T. A. et al., 2005, ApJ, 628, 453
Brustlein S., Del Rio L., Tonello A., Delage L., Reynaud F., Herrmann H., Sohler W., 2008, Phys. Rev. Lett., 100, 153903
Connes P., Reynaud F., 1988, in Fritz M., ed., European Southern Observatory Conference and Workshop Proceedings, Garching bei Munchen; Hamburg: European Southern Observatory (ESO), p. 1117, http://adsabs.harvard.edu/abs/1988ESOC...29.1117C, (accessed November 29, 2024)
Darré P. et al., 2016, Phys. Rev. Lett., 117, 233902
GRAVITY Collaboration, 2017, A&A, 602, A94
Gies D., Brummelaar T. t., Schaefer G., Baron F., White R., 2019, Bull. AAS, 51, 1
Gomes J.-T. et al., 2014, Phys. Rev. Lett., 112, 143904
Lawson P. R., 2000, in Lawson P. R., ed., Principles of Long Baseline Stellar Interferometry. Jet Propulsion Laboratory, La Cañada Flintridge, California, USA, p. 1, http://adsabs.harvard.edu/abs/2000plbs.conf.....L, (accessed November 29, 2024)
Le Bouquin J.-B. et al., 2011, 535, A67
Lehmann L. et al., 2018, Exp. Astron., 46, 447
Lehmann L. et al., 2019a, Exp. Astron., 47, 303
Lehmann L. et al., 2019b, MNRAS, 485, 3595
Ligon R. et al., 2022, in Mérand A., Sallum S., Sanchez-Bermudez J., eds, Vol. Proc. SPIE Conf. Ser. Vol. 12183, Optical and Infrared Interferometry and Imaging VIII. SPIE, Bellingham, p. 121832N
Magri J. et al., 2020, MNRAS, 501, 531
Magri J., Grossard L., Reynaud F., Fabert M., Delage L., Krawczyk R., Duigou J.-M. L., 2024, Exp. Astron., 57, 13
Mourard D. et al., 2018, in Mérand A., Creech-Eakman M. J., Tuthill P. G., eds, SPICA, a new 6T visible beam combiner for CHARA: science, design and interfaces, Optical and Infrared Interferometry and Imaging VI. SPIE, Bellingham, p. 1070120, https://www.spiedigitallibrary.org/conference-proceedings-of-spie/10701/2311869/SPICA-a-new-6T-visible-beam-combiner-for-CHARA/10.1117/12.2311869.full, (accessed November 29, 2024)
Perrin G. et al., 2006, Science, 311, 194
Reynaud F., Alleman J. J., Connes P., 1992, Appl. Opt., 31, 3736
Setterholm B. R. et al., 2023, J. Astron. Telesc. Instrum. Syst., 9, 025006
Shaklan S. B., Roddier F., 1987, Appl. Opt., 26, 2159
Szemendera L., Darré P., Baudoin R., Grossard L., Delage L., Herrmann H., Silberhorn C., Reynaud F., 2016, MNRAS, 457, 3115
ten Brummelaar T. A. et al., 2018, in Close L. M., Schreiber L., Schmidt D., eds, Proc. SPIE Conf. Ser. Vol. 10703, Adaptive Optics Systems VI. SPIE, Bellingham, 1070304
Vergnole S., Kotani T., Perrin G., Delage L., Reynaud F., 2005, Opt. Commun., 251, 115
Woillez J., Perrin G., Lai O., Coudé du Foresto V., Léna P., 2001. in Surdej J., Swings J. P., Caro D., Detal A., eds, OHANA: an optical Hawaiian array for nanoradian astronomy. Vol. 36, p. 139, http://adsabs.harvard.edu/abs/2001LIACo..36..139W, (accessed November 29, 2024)

APPENDIX A: ADDITIONAL FIGURES

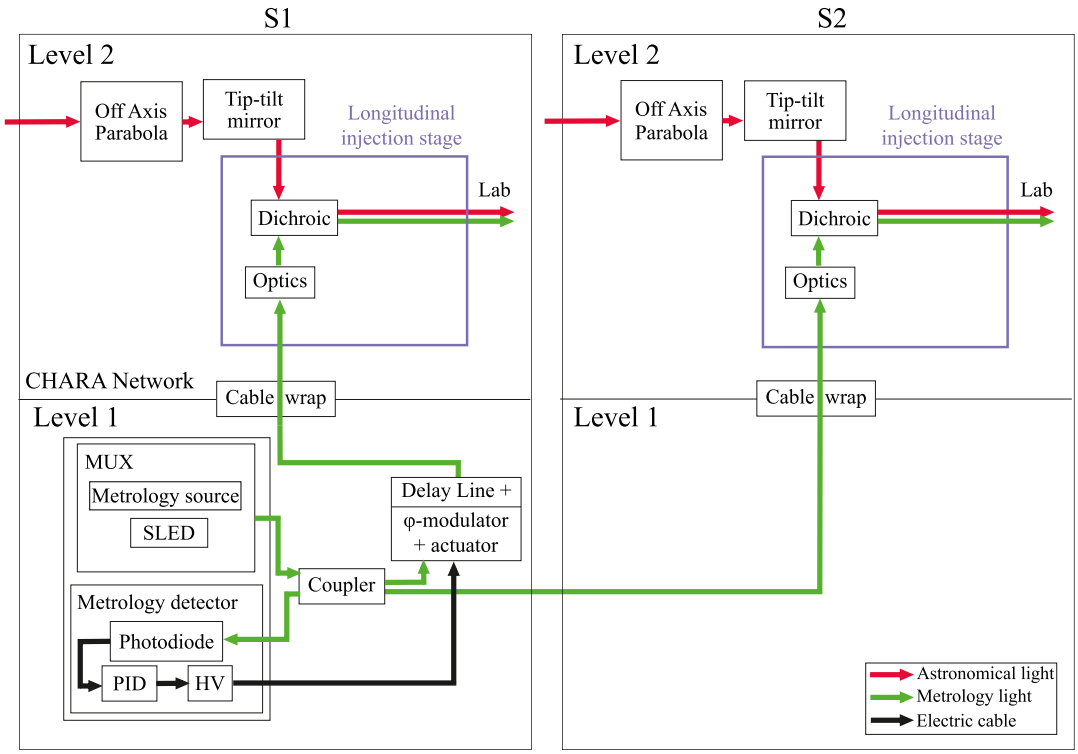

Figure A1. Overview diagram of the telescope's setup at CHARA for the ALOHA project. The astronomical light collected by the telescopes S1 and S2 and the 1064 nm metrology signal are both injected into two 240 m PM fibres going to the recombination laboratory. SLED: superluminescent diode (internal source), PID: proportional-integral-derivative controller, MUX: multiplexer, HV: high voltage amplifier, φ-modulator: phase modulator.

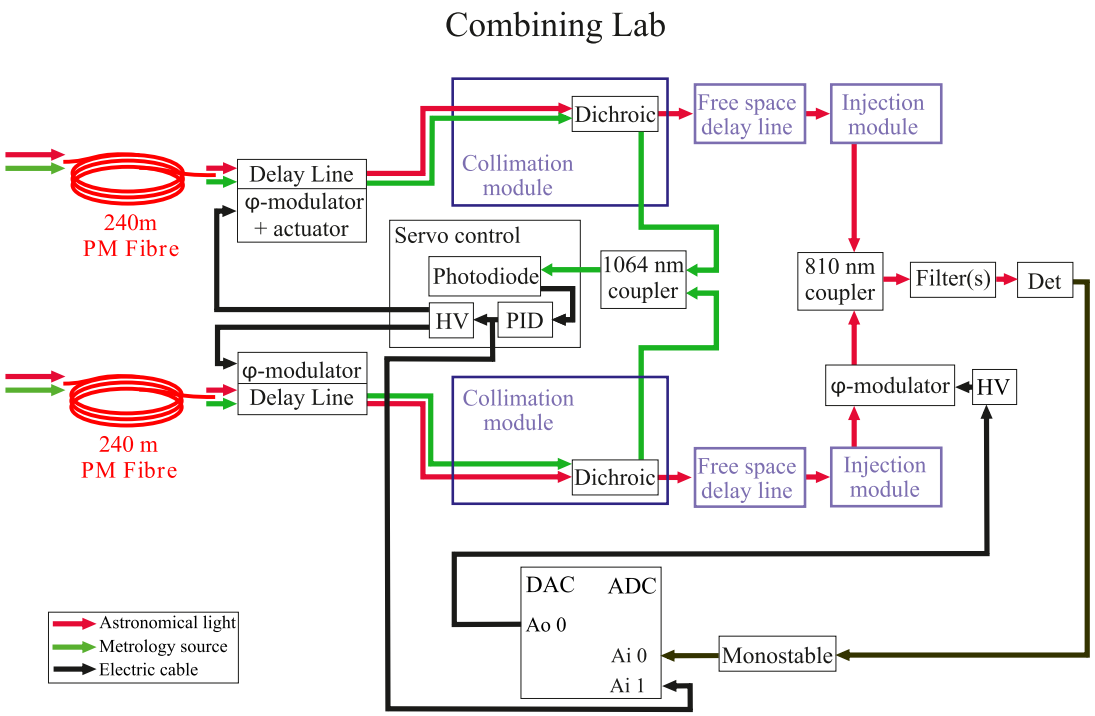

Figure A2. Overview diagram of the combining laboratory (mixing) set-up. The astronomical and metrology lights coming from the 240 m fibres pass through the collimation modules. The astronomical light around 810 nm travels through the free space CHARA delay lines and the 1064 nm signal is extracted for metrology purposes. Det: photon counting detector, DAC: digital-to-analogue converter, ADC: analogue to digital converter, Ao: analogue output, Ai n: analogue input channel n, PID: proportional-integral-derivative controller, HV: high voltage amplifier, φ-modulator: phase modulator. Note that in the future, a second photon counting detector can be added in order to enhance the signal-to-noise ratio.

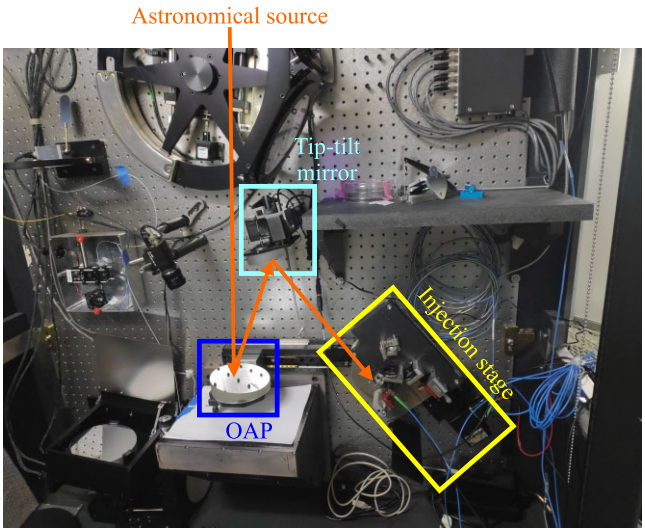

Figure A3. Picture of the injection stage in the telescope (S1 or S2). OAP: Off Axis Parabola.

This paper has been typeset from a TEX/LATEX file prepared by the author.